climate

MDPI

Article

Precipitation Extremes and Trends over the Uruguay River Basin in Southern South America

Vanessa Ferreira [1,2,*], Osmar Toledo Bonfim [1], Rafael Maroneze [1], Luca Mortarini [3], Roilan Hernandez Valdes [4] and Felipe Denardin Costa [1]

1 Pós-Graduação em Engenharia (PPEng), Universidade Federal do Pampa (UNIPAMPA), Av. Tiarajú 810, Alegrete 97546-550, Brazil; osmarbonfin@unipampa.edu.br (O.T.B.); rafaelmaroneze@unipampa.edu.br (R.M.); felipecosta@unipampa.edu.br (F.D.C.)
2 Departamento de Fisica, Universidade Federal de Santa Maria (UFSM), Av. Roraima 1000, Santa Maria 97105-900, Brazil
3 Institute of Atmospheric Sciences and Climate, National Research Council (ISAC-CNR), Corso Fiume 4, 10133 Torino, Italy; l.mortarini@isac.cnr.it
4 ENGIE Brasil Ernergia, Rua Paschoal Apóstolo Pítsica 5064, Florianópolis 88025-255, Brazil; roilan.valdes@engie.com
* Correspondence: vanessaferreira@unipampa.edu.br

Abstract: This study analyzes the spatial distribution and trends in five extreme daily rainfall indices in the Uruguay River Basin (URB) from 1993 to 2022 using the Climate Hazards Group Infrared Precipitation with Stations (CHIRPS) dataset. The main findings reveal a predominantly positive trend in heavy precipitation (R95p) and extreme precipitation (R99p) events over the mid URB, while a negative trend is observed in the upper and low URB. Significant trends in the frequency of heavy and extreme rainfall were observed during autumn (MAM), with positive trends across most of the mid and upper URB and negative trends in the low URB. In the upper URB, negative trends in the frequency of extremes were also found during spring (SON) and summer (DJF). Overall, there was a reduction in the number of consecutive wet days (CWD), particularly significant in the upper URB and the northern half of the mid URB. Additionally, the upper URB experienced an overall increase in the duration of consecutive dry days (CDD).

Keywords: extreme precipitation; precipitation trends; Uruguay river basin; southern South America

Citation: Ferreira, V.; Bonfim, O.T.; Maroneze, R.; Mortarini, L.; Valdes, R.H.; Costa, F.D. Precipitation Extremes and Trends over the Uruguay River Basin in Southern South America. *Climate* **2024**, *12*, 77. https://doi.org/10.3390/cli12060077

Academic Editor: Nir Y. Krakauer and Rui A. P. Perdigão

Received: 12 March 2024
Revised: 27 April 2024
Accepted: 11 May 2024
Published: 22 May 2024

1. Introduction

The Uruguay River Basin (URB) spans three South American countries: Brazil, Argentina, and Uruguay. It is part of the larger La Plata Basin and is the second main tributary of the La Plata River. Key economic activities in the region include agriculture, livestock farming, and hydroelectric power generation, all of which depend directly on rainfall. Additionally, an important hydrological feature of the URB is that the lag between river discharge and rainfall is small, which means that the basin is very responsive to precipitation events. When intense rainfall occurs, it can rapidly result in floods.

The region does not have a well-defined rainy season, and rainfall can be considered well-distributed throughout the year. Therefore, heavy precipitation events can occur all over the year ([1]). Consequently, cities along the Uruguay River are frequently affected by floods, resulting in significant social and economic impacts. One example is the flood that occurred in June 2014, affecting municipalities in northern Rio Grande do Sul (RS) and western Santa Catarina (SC). In the municipality of Iraí, located in northern RS, a monthly accumulated rainfall of 467 mm was recorded for June 2014. In this same municipality, the National Water Agency reported that the Uruguay River reached a level of 15 m, making it the third-highest level recorded in history since 1941. This flood event resulted in property damage, displacement of several people, substantial road damage, and incalculable financial losses for the agriculture and livestock sectors affected.

Similar to most of southeastern South America, the URB region experienced an overall positive trend in precipitation ([2–6]) and streamflow ([7,8]) during the late twentieth century. These positive trends in precipitation are in part associated with an increase in the intensity and frequency of heavy and extreme precipitation [3], which in turn, can greatly impact the URB. Therefore, understanding the spatial distribution and trends of extreme rainfall in the different regions of the basin may help minimize the adverse impacts of floods.

Over the past decades, although studies have investigated precipitation extremes and trends over the region, none have addressed specifically the URB. Most of the works looked at a more regional scale ([3,5,6]) or focused on the entire La Plata Basin ([9–11]). Other studies, such as [12,13], addressed only specific locations in the basin. Additionally, with the exception of [11], most studies used a limited number of precipitation stations or cluster analysis.

Therefore, in this study, we use daily precipitation data from the Climate Hazards Group Infrared Precipitation with Stations (CHIRPS) to analyze the spatial distribution and trends of extreme precipitation indices in the entire Uruguay River Basin (URB) during the recent 1993–2022 period. We will focus on five extreme daily precipitation indices defined by the Expert Team on Climate Change Detection and Indices (ETCCDI) because we are interested in analyzing only those indices more associated with extreme precipitation events, rather than trends in overall precipitation over the basin. Additionally, we will focus on the subregional scale patterns and trends in extreme precipitation indices across the URB.

2. Materials and Methods

2.1. Study Area

The Uruguay River Basin (URB) covers about 350,000 km^2 and spreads over three South American countries; Brazil, Argentina and Uruguay (Figure 1). To facilitate the discussion of results, the basin was subdivided into three main hydrographic regions: the upper URB, mid URB, and low URB. We used the hydrographic mesoregion division recommended by the Brazilian Institute of Geography and Statistics (IBGE, acronym in Portuguese) and the Brazilian National Water Agency (ANA, acronym in Portuguese), known as DHN25, which was launched in 2021. This division, developed by a team of experts from both IBGE and ANA, was established based on the homogeneity of geomorphological, hydrographic, and hydrological factors. Its primary objective is to facilitate the planning and efficient use of water resources in the region. The southernmost part of the basin is referred to as the low URB. The division between the mid and low URB follows the border between Uruguay and Brazil and is similar to the one used by [14].

The upper URB encompasses the northernmost part of the basin, where the Uruguay River originates. It is located in the Brazilian states of Santa Catarina (SC) and the northern region of Rio Grande do Sul (RS). This sector has a high potential for hydroelectric generation. Due to its steep topography and low soil capacity, it exhibits a rapid hydrological response to precipitation. The mid-URB is situated in western Rio Grande do Sul state, Brazil, and extends along the border with northeastern Argentina. The region transitions from steep terrain in the north to flat terrain in the Campanha Gaúcha region. The lower URB is located in western Uruguay and eastern Argentina. This region is characterized by flat terrain and is where the Uruguay River flows into the La Plata River after covering a distance of 2200 km from its source.

The local economy in this region is predominantly based on agriculture and livestock. The main annual crops include soybeans, wheat, maize, and rice, with rice plantations being the largest water consumers in mid-URB due to flood irrigation practices. In fact, Rio Grande do Sul state accounts for over 50% of Brazil's total rice production and is also a major contributor to agricultural crop production in the country. As seen in Figure 1, there are 14 hydropower plants in the basin nine of which have storage reservoirs: Garibaldi, Campos Novos, Barra Grande, Machadinho, Passo Fundo, and Quebra Queixo, Salto

Grande, Gabriel Terra, and Baygorria. Despite hydroelectric dams being used for flood control operations, persistent and intense rainfall events over the upper catchment, coupled with the low soil storage capacity and a rainfall-dependent flow regime, often lead to downstream flooding.

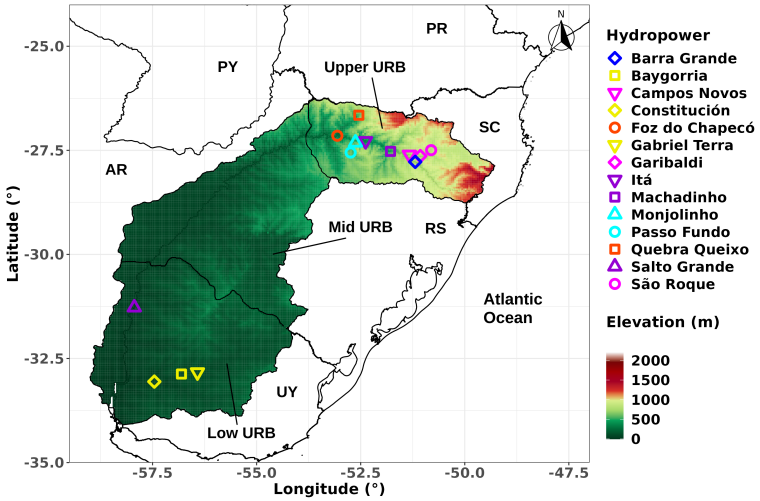

Figure 1. Topographic features of the Uruguay River Basin area, which is subdivided into three main hydrographic regions: the Upper URB, Mid URB, and Low URB. The acronyms are as follows: UY for Uruguay, AR for Argentina, PY for Paraguay, and the Brazilian states of RS for Rio Grande do Sul, SC for Santa Catarina, and PR for Paraná.

Figure 2 displays the monthly accumulated precipitation averaged for each of the three main hydrographic regions of the URB during the 1993–2022 period, calculated from daily precipitation data from CHIRPS. Overall, precipitation is well distributed across the entire URB throughout the year. Winter (from June to August) typically experiences the lowest rainfall amounts across the URB. The upper part of the basin receives more precipitation, ranging from 119 mm in August to 222 mm in October, while the lower part receives less, ranging from 87 mm in July to 171 mm in April, and the monthly accumulated rainfall in the mid-URB ranges from 98 mm in August up to 200 mm October.

While the monthly distribution of rainfall in the URB is generally uniform, day-to-day variability is high. Many extreme precipitation events are associated with the formation of Mesoscale Convective Systems ([15,16]). Additionally, the passage of cold fronts associated with extratropical cyclones serves as an important source of convective activity in the URB region ([1]). Furthermore, subtropical South America is recognized as one of the world's most active regions for severe convective storms ([17,18]). These convective storms can also generate high precipitation rates, leading to extreme events.

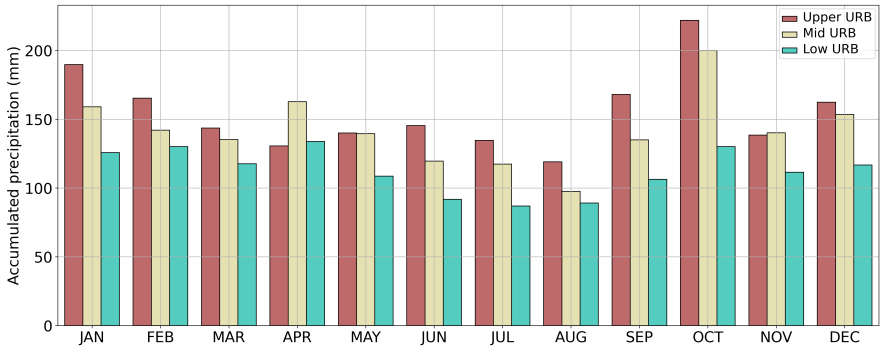

Figure 2. Monthly accumulated precipitation for the three main hydrographic regions of the Uruguay River Basin using CHIRPS data, and considering the 1993−2022 period.

2.2. Data Source, Precipitation Indices and Trends

Daily precipitation data were obtained from the CHIRPS version v2.0 dataset ([19]), comprising a 30-year period from 1993 to 2022. The CHIRPS database encompasses a quasi-global spatial domain (50° S–50° N, 180° E–180° W) at a spatial resolution of 0.05°, spanning from 1981 to the present. This dataset merges precipitation information from global climatology, satellite-based estimates, and in situ observations. Ref. [20] showed that the CHIRPS dataset adequately reproduces several characteristics of regional precipitation, capturing large-scale spatial patterns and variability at different timescales within the LPB. Therefore, it can serve as an alternative to precipitation data from surface stations.

The extreme precipitation indices recommended by the ETCCDI and used in this study are presented in Table 1. The indices were obtained for each pixel and on an annual-scale basis considering the 1993–2022 period.

For each precipitation index, linear regression analysis is applied to detect and analyze trends in the time series. The main statistical parameter drawn from the regression analysis is the slope, which indicates the mean temporal change in the studied variable. Positive values of the slope indicate increasing trends, while negative values indicate decreasing trends. In this work, trends were considered statistically significant at the p-value ≤ 0.05 level using Pearson correlation.

Table 1. Extreme daily precipitation indices used in this study.

Index	Indicator Name	Definition	Units
RX5day	Maximum 5-day precipitation amount	Monthly maximum consecutive 5-day precipitation	mm
CDD	Consecutive dry days	Maximum number of consecutive days with daily rainfall <1 mm	days
CWD	Consecutive wet days	Maximum number of consecutive days with daily rainfall ≥1 mm	days
R95p	Heavy precipitation	Annual total precipitation from daily rainfall >95th percentile	mm
R99p	Extreme precipitation	Annual total precipitation from daily rainfall >99th percentile	mm

3. Results and Discussion

Figure 3 shows the spatial distribution and trends of the R95p and R99p indices. R95p (Figure 3a) values range from 40 to 60 mm per day, with the mid-URB having the highest number of grid points with R95p above 55 mm. Conversely, the southern half of low URB and the eastern part of upper URB are the regions with the lowest R95p values. The spatial distribution of extreme precipitation thresholds, indicated by the R99p index (Figure 3b), is similar to that of R95p, but ranges from 50 to 90 mm/day.

The trends are predominantly positive and statistically significant for R95p (Figure 3c) across most of the mid-URB, with a maximum increase of around 4–5 mm per decade. Similarly, significant positive trends of 4 mm/decade for R99p are observed in the northern half of the mid-URB; however, negative trends are observed in the southern half. In the upper URB, the spatial distribution of trends is similar for both R95p and R99p. Significant positive trends are observed in the eastern end, while negative trends are noticeable in the northwestern sector. The low URB presents a less clear picture. R95p trends exhibit only a few statistically significant points, with no dominant signal observed. For R99p (Figure 3d), a negative trend is apparent across the entire low URB. The studies of [3,5,6,21], using rain gauge data, also identified overall positive trends in both annual total precipitation and extreme precipitation over the URB region in the last few decades.

The spatial distribution of the number of days with rainfall exceeding the threshold for the R95p index is presented in Figure 4, categorized by season. In the URB, the frequency of heavy rain days varies from approximately 10 to 60 days across seasons. During DJF (Figure 4a), the highest frequency occurs in the region along the border between RS state and Uruguay. In MAM (Figure 4b), the entire basin experiences a high number of heavy

rain days, ranging from 50 to 60 days. For JJA and SON (Figure 4c,d), a similar frequency of 50 to 60 days with heavy precipitation is observed, mainly in the upper URB and northern half of the mid-URB. In contrast, the rest of the basin experiences only 10 to 20 days with accumulated rainfall exceeding the R95p threshold during the 1993–2022 period.

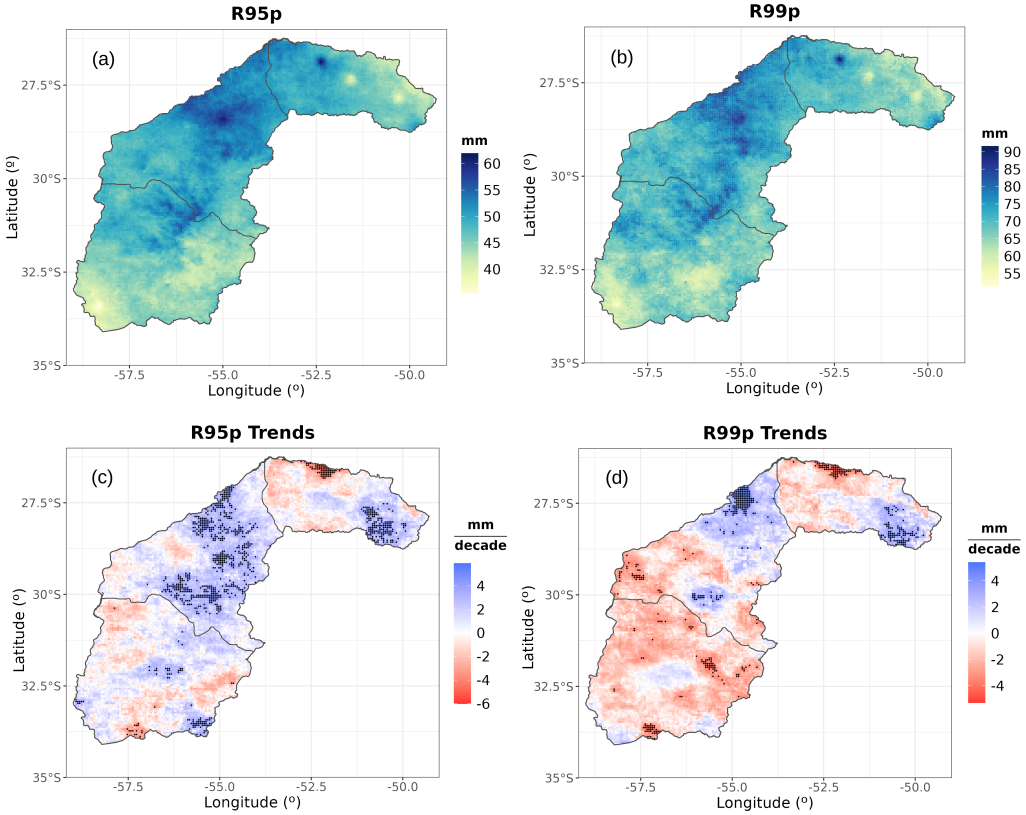

Figure 3. Spatial distribution of the extreme daily precipitation indices during the 1993−2022 period: (**a**) R95p and (**b**) R99p (mm). Trends of (**c**) R95p and (**d**) R99p in mm/decade during 1993–2022. Dark dots are grid points with significant trends at the 95% significance level. The continuous lines distinguish hydrographic regions of the Uruguay River Basin shown in Figure 1.

A similar spatial distribution is observed for the number of days with precipitation exceeding the R99p threshold, as depicted in Figure 5. However, extreme precipitation events are rarer than heavy precipitation, with the number of days with rain reaching the R99p percentile ranging from 2 to 20 days, compared to 10 to 60 days per season for R95p. The frequency of extreme precipitation during MAM (Figure 5b) is high and relatively uniform across the entire URB. During DJF (Figure 5a), the amount of extreme events is higher over the southern half of the basin. In JJA and SON (Figure 5c,d), more extreme precipitation days are observed over the upper URB, especially in JJA.

Figure 6 shows the trends associated with the number of days above the R95p threshold for each season. Within the low URB, a predominantly positive trend is observed during DJF, JJA, and SON (Figure 6a,c,d), indicating an increasing frequency of heavy precipitation events during the 1993–2022 period. Conversely, during MAM (Figure 6b), a decreasing trend in the number of days with heavy precipitation is detected across the majority of the low URB region. However, statistically significant trends are observed in only a few grid points, and their locations vary among the seasons.

In all seasons, a significant positive trend of R95p (Figure 6) is observed in the eastern sector of the upper URB, between longitudes −51° to −50°. Additionally, an overall increasing trend extends across the majority of the upper URB during MAM (Figure 6b). Conversely, in the remaining area of the upper URB during DJF and SON (Figure 6a,d), significant negative trends predominate, particularly in SON. A decrease in the frequency

of extreme rainfall events during DJF was also observed by [13] for Santa Catarina state, which encompasses most of the upper URB. However, they found an increase in frequency during SON. No clear and significant trend is detected in JJA. Across most of the mid-URB, a statistically significant positive trend is observed during MAM (Figure 6b). However, for the remaining seasons, no clear and significant trend is detected. Only the northern sector, near the border with the upper URB, exhibits statistically significant negative trends during DJF and SON (Figure 6a,d).

Looking at the trends in the number of days with rainfall above the R99p value, as depicted in Figure 7, a statistically significant negative trend is observed in MAM (Figure 7b) within the low URB, indicating a decrease in the frequency of extreme precipitation events. Similarly, although with fewer statistically significant grid points, a decreasing trend is observed in JJA (Figure 7c), except for the southern strip of the low URB where positive trends are detected. Conversely, in the same southern strip, negative trends are observed during SON (Figure 7d), with the remaining region showing no statistical significance. In DJF (Figure 7a), negative trends are observed in the northern half of the low URB, but with just a few grid points displaying statistical significance.

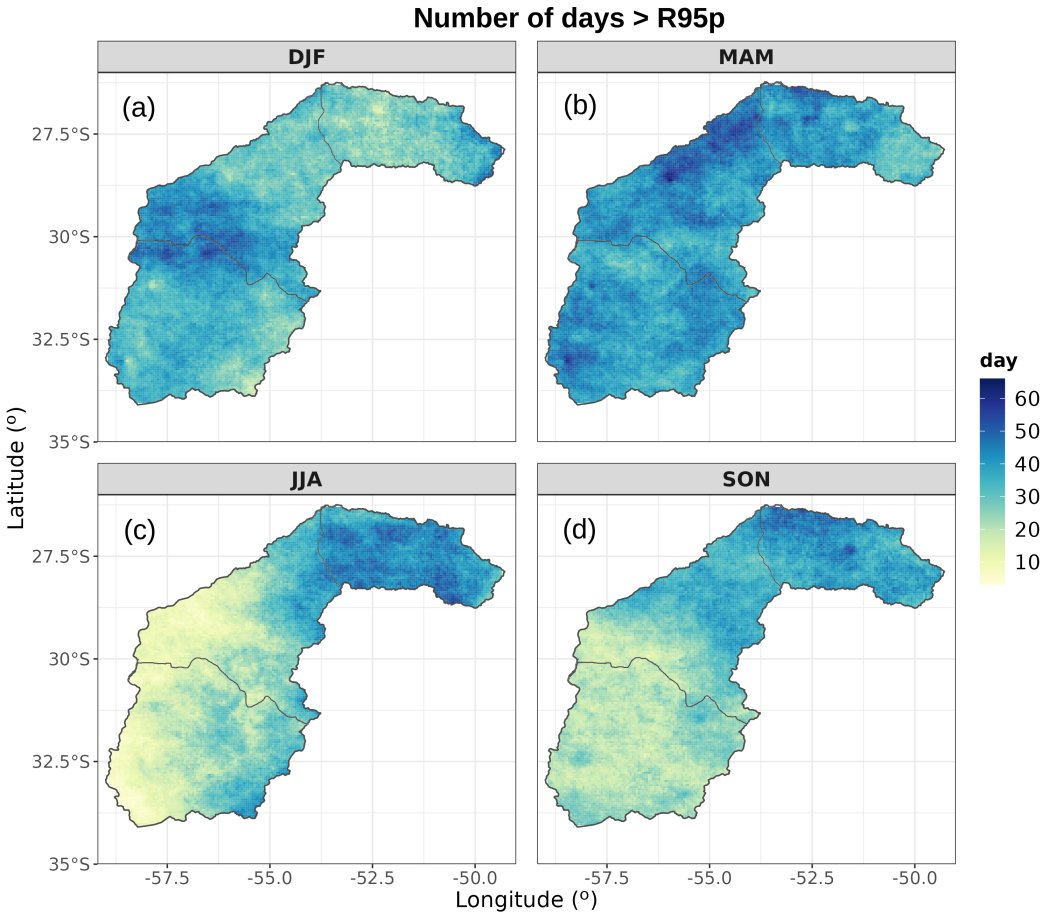

Figure 4. Spatial distribution of the number of days with precipitation above the R95p threshold during (**a**) DJF (December−January−February months; austral summer), (**b**) MAM (March−April−May trimester; austral autumn), (**c**) JJA (June−July−August months; austral winter) and (**d**) SON (September−October−November; austral spring). The continuous lines distinguish hydrographic regions of the Uruguay River Basin shown in Figure 1.

In the mid-URB, once again, the most significant trends are observed in MAM (Figure 7b), showing an overall increasing trend, especially over the northwestern sector. During SON (Figure 7d), an overall negative trend is observed. Additionally, the area centered around longitude −55° and latitude −29.5° exhibits a significant negative

trend in JJA (Figure 7c) and a positive trend in DJF (Figure 7a). Conversely, the region just to the north, while showing few statistically significant points, displays positive trends in JJA and negative trends in DJF. In the upper URB, statistically significant trends are observed in just a few grid points in all seasons. Nevertheless, an overall positive trend is evident during MAM and JJA (Figure 7b,c), whereas a decreasing trend is observed during SON (Figure 7d), with no clear signal apparent in DJF (Figure 7a).

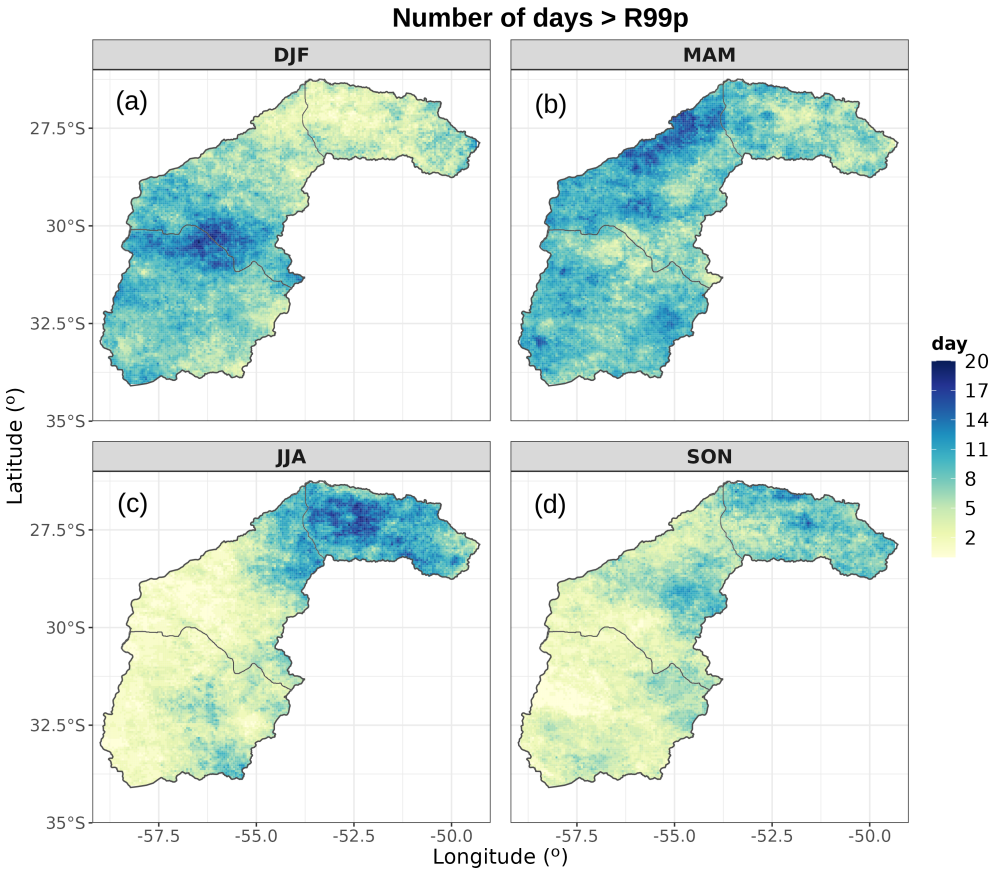

Figure 5. Spatial distribution of the number of days with precipitation above the R99p threshold during (**a**) DJF (December−January−February months; austral summer), (**b**) MAM (March−April−May trimester; austral autumn), (**c**) JJA (June−July−August months; austral winter) and (**d**) SON (September−October−November; austral spring). The continuous lines distinguish hydrographic regions of the Uruguay River Basin shown in Figure 1.

Figure 8 displays the spatial distribution and trends of RX5day, which is the maximum precipitation amount in five consecutive days during the 1993–2022 period. The highest values of RX5day are observed in the region around the border between the mid and upper URB, reaching approximately 350-400 mm. However, for the majority of the basin, RX5day values vary from 200 to 300 mm (Figure 8a). Statistically significant trends were found only for a few grid points (Figure 8b). However, overall, there are negative trends over the majority of the upper URB sector, except for the eastern end where positive trends are observed. In the mid-URB, mostly positive trends are observed. Conversely, mostly negative trends are observed over the northern half of the low URB, while positive trends are seen in the southern half. This spatial distribution of Rx5day trends is similar to those for R95p and R99p.

Figure 9 presents the maximum annual duration of dry and wet spells, characterized by the consecutive dry and wet days indices (CDD and CWD), considering the period from 1993 to 2022. Across the URB, wet spells last from 6 to 21 days (Figure 9a). In Figure 9b, mostly negative trends are observed in the URB, indicating a decrease in wet spell duration

over the last three decades. These negative trends are more significant in the upper URB, the northern half of the mid-URB, and the northeastern end of the low URB, with a decrease of up to –5 days per decade in CWD duration. Ref. [11], in their analysis of the entire La Plata Basin, also observed a similar pattern of CWD trends in the URB region.

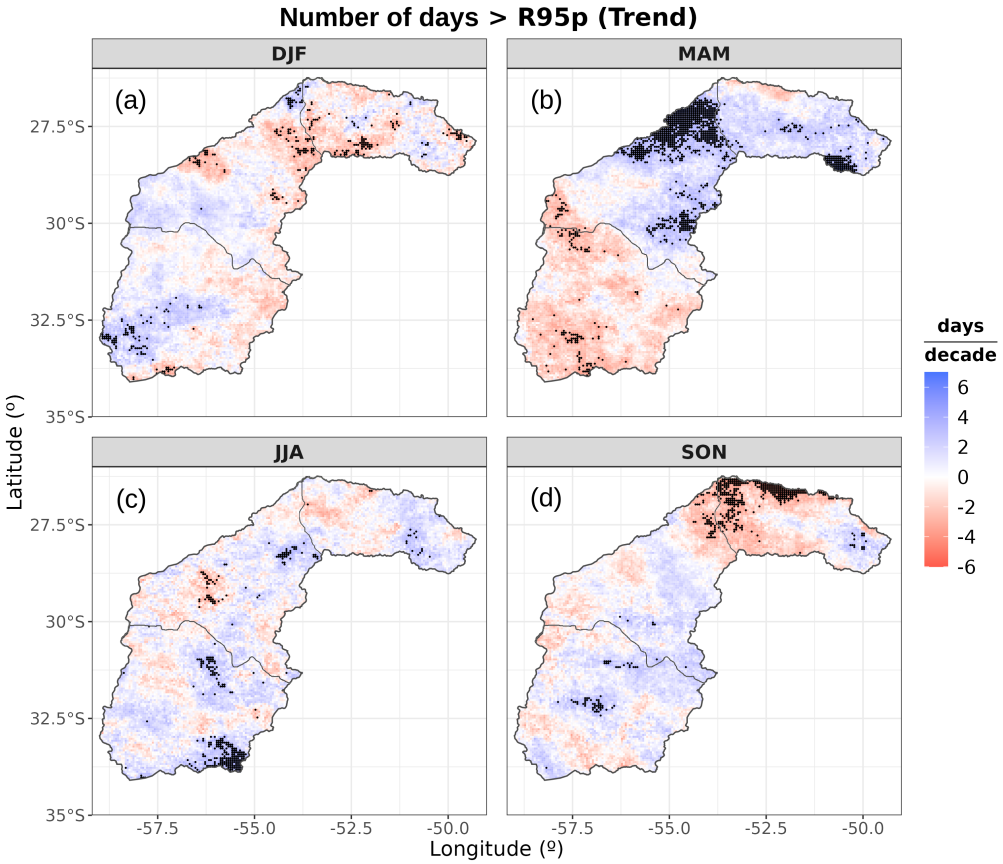

Figure 6. Trends on the number of days with precipitation above the R95p threshold during (**a**) DJF (December−January−February months; austral summer), (**b**) MAM (March−April−May trimester; austral autumn), (**c**) JJA (June−July−August months; austral winter) and (**d**) SON (September−October−November; austral spring). Dark dots are grid points with significant trends at the 95% significance level. The continuous lines distinguish hydrographic regions of the Uruguay River Basin shown in Figure 1.

The spatial distribution of dry spells is presented in Figure 9c, showing that they last from around 30 to 55 days. Regarding CDD trends, Figure 9d shows statistically significant negative trends of up to –5 days per decade in the overall northern half of the low URB, and positive trends, although with fewer significant grid points, in the southern half of low URB. For the mid and upper URB, there seems to be an overall positive CDD trend. [3] also found mostly upward trends in CDD in southern South America.

As shown in Figure 1, the majority of hydropower plants are located in the upper URB; the results shown above indicate that in this region there is mostly a decreasing trend in the intensity of extreme and heavy rain. Negative trends are also observed in the frequency of these events during SON and DJF, while an increase in frequency is observed during MAM. Additionally, the results indicate a reduction in the number of consecutive wet days (Figure 9b) and, an increase in consecutive dry days (Figure 9d) in the entire upper URB. Therefore, these results can have a significant impact on hydroelectric generation, not only in this region but also at the national and international level, as these hydroelectric dams provide energy nationwide and for neighboring countries such as Argentina and Uruguay.

Extreme precipitation events contribute to reservoir filling, so a reduction in such events may lead to lower water availability for hydropower generation. This reduction can

result in a decrease in energy production from hydropower plants in the upper URB. The impact of this reduction may be more pronounced during SON and DJF, as not only the intensity but also the frequency of heavy and extreme precipitation events decreases during these seasons. Furthermore, the increase in prolonged periods without rainfall (CDD) can elevate the risk of drought conditions, further impacting water availability for hydropower generation, agricultural activities, and water supply in the region. However, this region, characterized by steep topography and low soil storage capacity, is prone to rapid flooding when intense rainfall occurs. Consequently, the observed decreasing trend in the frequency and intensity of heavy and extreme precipitation events can decrease flood risk and its socioeconomic impacts, both within this sector of the basin and downstream.

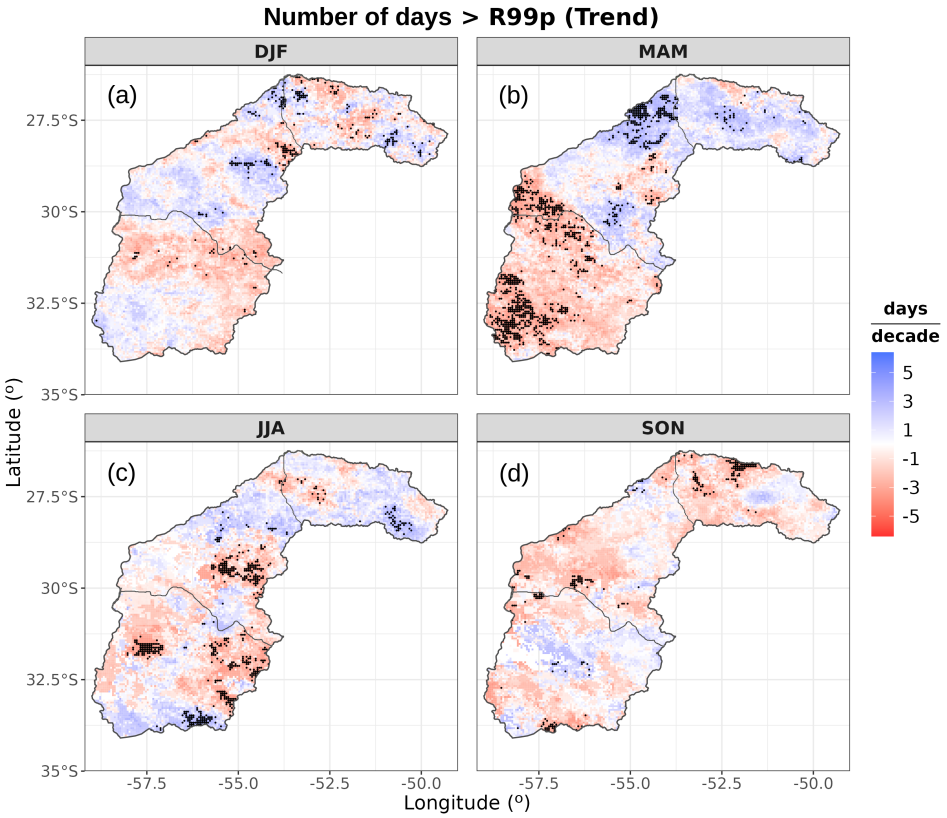

Figure 7. Trends on the number of days with precipitation above the R99p threshold during (**a**) DJF (December−January−February months; austral summer), (**b**) MAM (March−April−May trimester; austral autumn), (**c**) JJA (June−July−August months; austral winter) and (**d**) SON (September−October−November; austral spring). Dark dots are grid points with significant trends at the 95% significance level. The continuous lines distinguish hydrographic regions of the Uruguay River Basin shown in Figure 1.

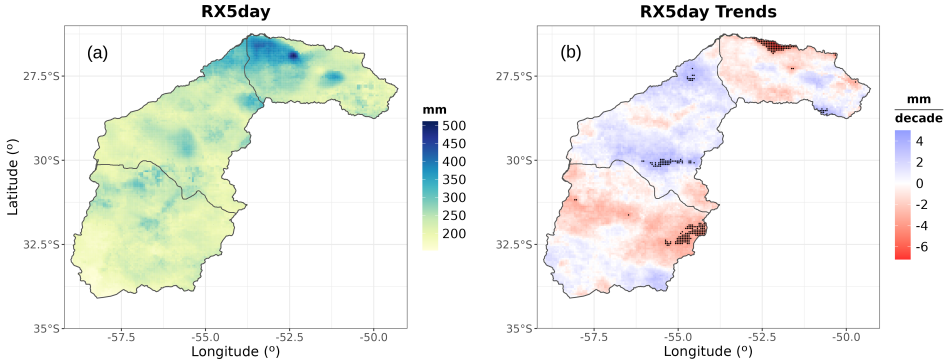

Figure 8. (**a**) Spatial distribution of maximum 5−day precipitation amount (RX5day) and (**b**) trends of annual time series of RX5day, during 1993−2022. Dark dots are significant trends at the 95% significance level. The continuous lines distinguish hydrographic regions of the Uruguay River Basin shown in Figure 1.

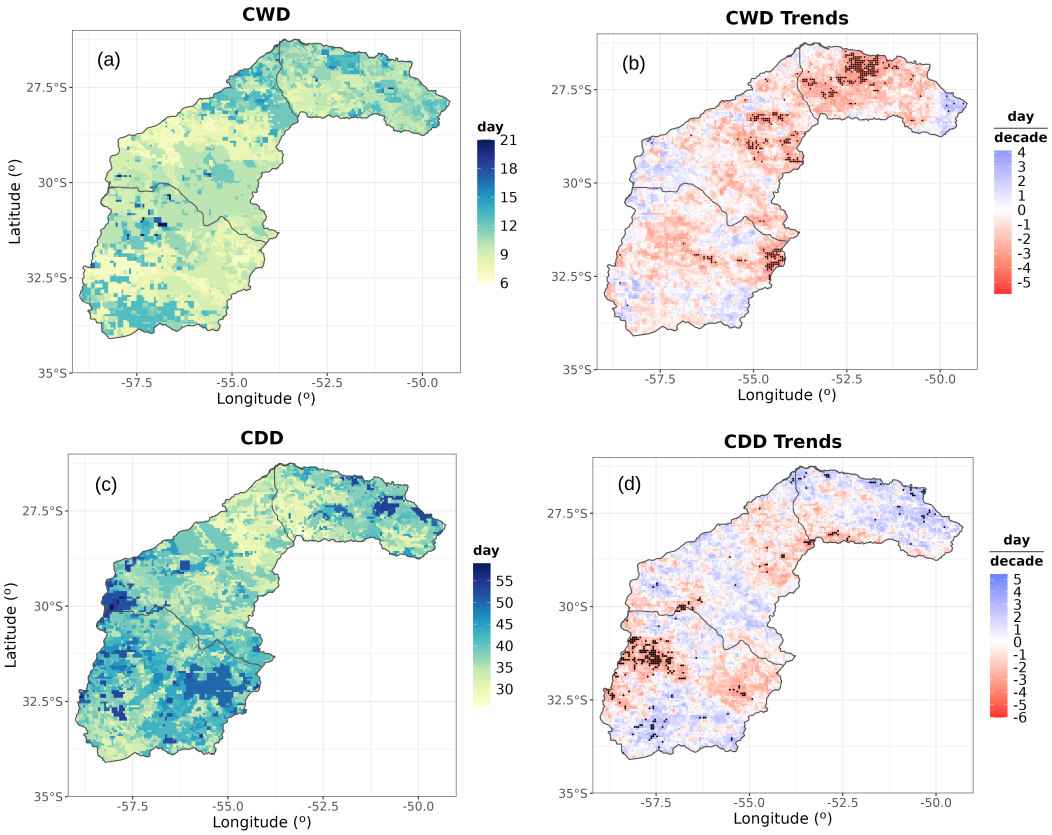

Figure 9. Spatial distribution and trends of annual time series of extreme precipitation indices during the 1993–2022 period: (**a**) wet spells (consecutive wet days; CWD), (**b**) CWD trends in a day per decade, (**c**) dry spells (consecutive dry days CDD), and (**d**) CDD trends in a day per decade. Dark dots are significant trends at the 95% significance level. The continuous lines distinguish hydrographic regions of the Uruguay River Basin shown in Figure 1.

Similar to the upper URB, the lower URB also shows an overall negative trend in extreme precipitation (R99p) and consecutive wet days (CWD). Additionally, unlike the rest of the basin, the lower URB has experienced a significant negative trend in extreme precipitation frequency during autumn (MAM; see Figure 6b). As depicted in Figure 1, this region also hosts hydroelectric plants, including the Salto Grande dam, which is one of the major hydropower plants in the La Plata Basin and is operated by Uruguay and Argentina.

Therefore, the discussion regarding the impact of reduced intensity and frequency of heavy rainfall on hydroelectric generation also applies to the low URB.

In contrast, heavy precipitation is intensifying throughout the mid URB (Figure 3c). The frequency of both heavy and extreme precipitation events shows a significant positive trend during autumn (MAM; Figures 6b and 7b). A mostly positive trend is also observed for prolonged and intense precipitation events (Rx5day). However, the duration of wet spells is decreasing (Figure 9b), and there is no clear trend in CDD. In this sector of the URB, agricultural activity serves as the primary economic driver with intensive use of water resources for rice irrigation.

While sufficient water availability benefits crops, an increase in the intensity of heavy precipitation can elevate the risk of flooding. This flooding, in turn, can lead to crop damage, soil erosion, waterlogging, and disruptions to planting and harvesting schedules, ultimately affecting crop yields and food security. Moreover, flooding can also have significant impacts on urban areas, including infrastructure damage, property loss, and disruptions to essential services. In fact, ref. [22] shows that municipalities along the mid-Uruguay River in the Rio Grande do Sul state have among the highest number of registered floodings in the region, with some cities experiencing up to 39 flooding episodes between 1980 and 2005.

A limitation of this study is that it relies solely on precipitation data from CHIRPS, without analyzing in situ precipitation and streamflow measurements to assess the quality of CHIRPS data. Additionally, a more comprehensive examination of rainfall extremes trends and patterns in the URB would ideally involve comparing various gridded products.

Furthermore, there are inherent limitations in satellite precipitation estimates, such as the difficulty in capturing extreme precipitation events, which often exhibit high spatial and temporal variability. Nevertheless, ref. [20] demonstrated that CHIRPS was able to capture precipitation patterns in the LBP. Additionally, CHIRPS has been utilized to evaluate precipitation extremes in other regions of South America ([23–25]) and also in the LPB ([11]). There are also limitations due to temporal inhomogeneity resulting from changes in the surface observing network, satellite instruments, and calibration and bias correction methods. Few studies have analyzed changes in the effectiveness of precipitation estimates over time. Regarding the CHIRPS dataset, studies by [26] for mainland China and [27] for the Koshi basin, Nepal, have shown that there are temporal inconsistencies in CHIRPS estimates for these regions.

4. Conclusions

In this study, the analysis focused on rainfall extremes in the Uruguay River Basin (URB) during the 1993–2022 period using five extreme daily climate indices recommended by the ETCCDI and the CHIRPS dataset, version 2.0. The URB was divided into three hydrographic regions: upper URB, mid URB, and low URB.

In the upper URB, the combination of a mostly negative trend in both heavy and extreme precipitation, along with a positive trend in consecutive dry days (CDD), indicates a transition towards drier conditions given the reduced intensity in precipitation extremes and more prolonged dry periods. Furthermore, there has been a decreasing trend in the frequency of precipitation extremes during spring and summer in the upper URB, while an increasing trend was observed during autumn. An overall upward trend in extreme rainfall was also observed in the low URB, with a significant decrease in the number of extreme rainfall days in autumn. These findings raise concerns regarding hydroelectric generation in the basin, particularly given that hydropower plants are located in both the upper and low URB sectors. These hydropower plants not only contribute to the local energy supply but also to other regions in Brazil, Argentina, and Uruguay.

The results also indicate that the mid-URB has been experiencing an increase in the intensity of heavy and extreme precipitation, along with an increase in the frequency of these events during autumn. This result points to an increase in the risk of flooding in the sector of the basin, impacting agricultural activities and urban areas in the region.

This study contributes to the existing literature on precipitation extremes trends in southeastern South America by addressing sub-regional trends in the URB, filling a gap that previous large-scale studies had overlooked. The precipitation extremes showed heterogeneous changes that did not indicate a characteristic pattern in the entire basin.

Author Contributions: Conceptualization, V.F.; methodology, V.F. and O.T.B.; software, O.T.B., R.M. and V.F.; formal analysis, V.F., O.T.B. and R.M.; resources, R.H.V.; writing-original draft preparation, V.F.; writing-review and editing, O.T.B., R.M. and F.D.C.; supervision, R.M., L.M. and R.H.V. All authors have read and agreed to the published version of the manuscript.

Funding: This research was funded by ENGIE Brasil Energia and Companhia Energética Estreito grant number P&D-00403-0054/2022.

Data Availability Statement: All datasets used in this study are available on public online databases. CHIRPS v2.0 dataset is available at https://www.chc.ucsb.edu/data/chirps/ (accessed on November 2023).

Acknowledgments: This research results from the R&D Project from ENGIE Brasil Energia and Companhia Energética Estreito (R&D-00403-0054/2022), and regulated by National Electric Energy Agency (ANEEL).

Conflicts of Interest: The funders had no role in the design of the study; in the collection, analyses, or interpretation of data; in the writing of the manuscript; or in the decision to publish the results.

References

1. Teixeira, M.S.; Satyamurty, P. Dynamical and synoptic characteristics of heavy rainfall episodes in southern Brazil. *Mon. Weather. Rev.* **2007**, *135*, 598–617. [CrossRef]
2. Liebmann, B.; Vera, C.S.; Carvalho, L.M.; Camilloni, I.A.; Hoerling, M.P.; Allured, D.; Barros, V.R.; Báez, J.; Bidegain, M. An observed trend in central South American precipitation. *J. Clim.* **2004**, *17*, 4357–4367. [CrossRef]
3. Haylock, M.R.; Peterson, T.C.; Alves, L.M.; Ambrizzi, T.; Anunciação, Y.; Báez, J.; Barros, V.R.; Berlato, M.; Bidegain, M.; Coronel, G.; et al. Trends in total and extreme South American rainfall in 1960–2000 and links with sea surface temperature. *J. Clim.* **2006**, *19*, 1490–1512. [CrossRef]
4. Barros, V.R.; Doyle, M.E.; Camilloni, I.A. Precipitation trends in southeastern South America: Relationship with ENSO phases and with low-level circulation. *Theor. Appl. Climatol.* **2008**, *93*, 19–33. [CrossRef]
5. Teixeira, M.d.S.; Satyamurty, P. Trends in the frequency of intense precipitation events in southern and southeastern Brazil during 1960–2004. *J. Clim.* **2011**, *24*, 1913–1921. [CrossRef]
6. Regoto, P.; Dereczynski, C.; Chou, S.C.; Bazzanela, A.C. Observed changes in air temperature and precipitation extremes over Brazil. *Int. J. Climatol.* **2021**, *41*, 5125–5142. [CrossRef]
7. Saurral, R.I.; Barros, V.R.; Lettenmaier, D.P. Land use impact on the Uruguay River discharge. *Geophys. Res. Lett.* **2008**, *35*. [CrossRef]
8. Pasquini, A.I.; Depetris, P.J. Discharge trends and flow dynamics of South American rivers draining the southern Atlantic seaboard: An overview. *J. Hydrol.* **2007**, *333*, 385–399. [CrossRef]
9. Doyle, M.E.; Saurral, R.I.; Barros, V.R. Trends in the distributions of aggregated monthly precipitation over the La Plata Basin. *Int. J. Climatol.* **2012**, *32*, 2149–2162. [CrossRef]
10. Penalba, O.C.; Robledo, F.A. Spatial and temporal variability of the frequency of extreme daily rainfall regime in the La Plata Basin during the 20th century. *Clim. Chang.* **2010**, *98*, 531–550. [CrossRef]
11. Ceron, W.L.; Kayano, M.T.; Andreoli, R.V.; Avila-Diaz, A.; Ayes, I.; Freitas, E.D.; Martins, J.A.; Souza, R.A. Recent intensification of extreme precipitation events in the La Plata Basin in Southern South America (1981–2018). *Atmos. Res.* **2021**, *249*, 105299. [CrossRef]
12. Ávila, A.; Justino, F.; Wilson, A.; Bromwich, D.; Amorim, M. Recent precipitation trends, flash floods and landslides in southern Brazil. *Environ. Res. Lett.* **2016**, *11*, 114029. [CrossRef]
13. Fernandes, L.G.; Rodrigues, R.R. Changes in the patterns of extreme rainfall events in southern Brazil. *Int. J. Climatol.* **2017**, *38*, 1337–1352. [CrossRef]
14. Armoa, O.L.; Sauvage Barresi, S.; Houska, T.; Bieger, K.; Schürz, C.; Sánchez Pérez, J.M. Representation of Hydrological Components under a Changing Climate—A Case Study of the Uruguay River Basin Using the New Version of the Soil and Water Assessment Tool Model (SWAT+). *Water* **2023**, *15*, 2604. [CrossRef]
15. Velasco, I.; Fritsch, J.M. Mesoscale convective complexes in the Americas. *J. Geophys. Res. Atmos.* **1987**, *92*, 9591–9613. [CrossRef]
16. Durkee, J.D.; Mote, T.L. A climatology of warm-season mesoscale convective complexes in subtropical South America. *Int. J. Climatol. J. R. Meteorol. Soc.* **2010**, *30*, 418–431. [CrossRef]

17. Zipser, E.J.; Cecil, D.J.; Liu, C.; Nesbitt, S.W.; Yorty, D.P. Where are the most intense thunderstorms on Earth? *Bull. Am. Meteorol. Soc.* **2006**, *87*, 1057–1072. [CrossRef]
18. Cecil, D.J.; Blankenship, C.B. Toward a global climatology of severe hailstorms as estimated by satellite passive microwave imagers. *J. Clim.* **2012**, *25*, 687–703. [CrossRef]
19. Funk, C.; Peterson, P.; Landsfeld, M.; Pedreros, D.; Verdin, J.; Shukla, S.; Husak, G.; Rowland, J.; Harrison, L.; Hoell, A.; et al. The climate hazards infrared precipitation with stations—A new environmental record for monitoring extremes. *Sci. Data* **2015**, *2*, 1–21. [CrossRef]
20. Cerón, W.L.; Molina-Carpio, J.; Ayes Rivera, I.; Andreoli, R.V.; Kayano, M.T.; Canchala, T. A principal component analysis approach to assess CHIRPS precipitation dataset for the study of climate variability of the La Plata Basin, Southern South America. *Nat. Hazards* **2020**, *103*, 767–783. [CrossRef]
21. Skansi, M.d.l.M.; Brunet, M.; Sigró, J.; Aguilar, E.; Groening, J.A.A.; Bentancur, O.J.; Geier, Y.R.C.; Amaya, R.L.C.; Jácome, H.; Ramos, A.M.; et al. Warming and wetting signals emerging from analysis of changes in climate extreme indices over South America. *Glob. Planet. Chang.* **2013**, *100*, 295–307. [CrossRef]
22. Reckziegel, B.W. Levantamento dos desastres desencadeados por eventos naturais adversos no estado do Rio Grande do Sul no período de 1980 a 2005. 2007. Avaliable online: https://www.oasisbr.ibict.br/vufind/Record/UFSM-20_62dcbddc53875330e327de59e65a8bd2 (accessed on 11 March 2024) .
23. Paca, V.H.d.M.; Espinoza-Dávalos, G.E.; Moreira, D.M.; Comair, G. Variability of trends in precipitation across the Amazon River basin determined from the CHIRPS precipitation product and from station records. *Water* **2020**, *12*, 1244. [CrossRef]
24. Cavalcante, R.B.L.; da Silva Ferreira, D.B.; Pontes, P.R.M.; Tedeschi, R.G.; da Costa, C.P.W.; de Souza, E.B. Evaluation of extreme rainfall indices from CHIRPS precipitation estimates over the Brazilian Amazonia. *Atmos. Res.* **2020**, *238*, 104879. [CrossRef]
25. Olmo, M.E.; Bettolli, M.L. Extreme daily precipitation in southern South America: Statistical characterization and circulation types using observational datasets and regional climate models. *Clim. Dyn.* **2021**, *57*, 895–916. [CrossRef]
26. Bai, L.; Shi, C.; Li, L.; Yang, Y.; Wu, J. Accuracy of CHIRPS satellite-rainfall products over mainland China. *Remote Sens.* **2018**, *10*, 362. [CrossRef]
27. Shrestha, N.K.; Qamer, F.M.; Pedreros, D.; Murthy, M.; Wahid, S.M.; Shrestha, M. Evaluating the accuracy of Climate Hazard Group (CHG) satellite rainfall estimates for precipitation based drought monitoring in Koshi basin, Nepal. *J. Hydrol. Reg. Stud.* **2017**, *13*, 138–151. [CrossRef]